

Three-dimensional strain softening modeling of deep longwall coal mine layouts

S. Badr, U. Ozbay, S. Kieffer & M. Salamon
Colorado school of mines, Golden, Colorado, USA

ABSTRACT: This paper describes a $FLAC^{3D}$ model for a typical deep two-entry longwall coal mine. The coal seam is modeled as a strain softening material to attain a representative analysis of stresses and deformations experienced by the coal ribs and yielding chain pillars corresponding to various loading stages. The strain softening parameters are established by calibrating separate test pillar models to common empirical pillar strength formulas. The test pillar models showed that strain softening material behavior results in lower pillar strengths than the traditional Mohr-Coulomb models based on constant peak cohesion and friction values. The longwall model incorporates compaction simulations of the gob material in the back area. Two algorithms for representing gob compaction are described.

1. INTRODUCTION

In mining practices, it is common for the induced loading to exceed the strength of the rock mass. Realistic representation of stresses and deformations in such situations requires use of constitutive laws that can account for the response of the rock mass in the post-peak state. Mohr - Coulomb (MC) and Hoek & Brown (HB) plasticity models are commonly used in these situations. Considering the brittle nature of many rock masses, strain softening type models, such as the Mohr-Coulomb Strain Softening (MCSS) option in $FLAC^{3D}$ (Itasca 2002), allow more realistic modeling of rock mass failure.

A typical mining situation where the modeling of brittle behavior becomes important is the analysis of yielding chain pillars in deep longwall mines. At depths more than about 300 m, the vertical stress exceeds the strength of unconfined coal, resulting in failure of the excavation walls while they are being exposed. This can result in the sides of entry pillars failing before the pillars are fully isolated. Realistic estimation of the loads carried by these pillars during subsequent mining requires the use of a softening model.

The longwall mining geometry and the sequence of excavation considered in this study are illustrated in a plan view in Figure 1. Three longwall panels

are shown in this illustration. The upper panel is already extracted. The panel at the bottom of the illustration has been developed, but extraction has not yet commenced. As the longwall face in the middle panel moves from right to left as indicated, the chain pillars undergo five stages of loading. These stages are indicated in the diagram; the first three affect the pillars next to the head gate and the last two affect the pillars next to the tailgate. Stage 1 corresponds to the situation where the entry-pillar system is fully developed, but the extraction of the longwall panels has not yet affected the loading of the pillar. Stage 2 refers to the situation where the front and side abutments contribute to the pillar loading due to the approaching longwall face.

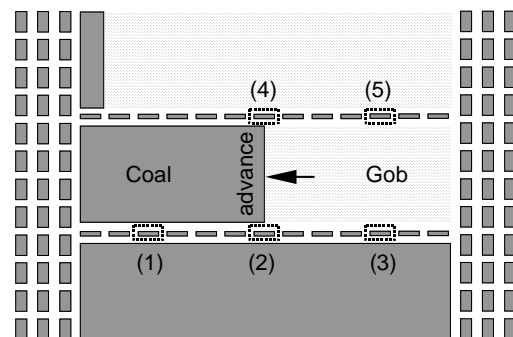


Figure 1. Simplified plan view of a two-entry longwall mine layout showing pillar loading stages.

In Stage 3, the gob on one side, and an unmined panel on the opposing side, affect the loading. The gob in the vicinity of the development is not fully compacted so it does not support the full weight of the overburden. In Stage 4 on the tailgate side, as the face approaches, the front abutment increasingly contributes to loading of the pillar; hence the conditions around the tailgate pillars become progressively more adverse. Stage 5 corresponds to the situation where the influence of the face is no longer detectable and the chain pillars are surrounded on both sides by gobs.

This paper describes a numerical model for assessing the longwall mining scenario described above. The coal seam is modeled as a MCSS material. A separate series of numerical analyses was carried out on a single pillar (test pillar model) to determine representative MCSS strength parameters for the coal seam. The test pillar model analysis was also performed with MC materials to permit comparison of the pillar response based on MC and MCSS behavior.

Compaction of the fractured, particulate material, called the “gob”, created by the caving of the roof in the area from where the coal has been extracted, requires attention in the numerical modeling of longwall mining. With continuing extraction, the upper strata and the floor converge and gradually the vertical load on the gob material increases. Representation of this process requires consideration of the deformations of both the gob materials and the surrounding strata. This paper describes two alternative algorithms to simulate gob compaction.

2. LONGWALL MODEL

The modeled longwall layout is similar to that shown in Figure 1. It represents a two-entry longwall mine located at a depth of 680 m below surface. The panel length is 220 m and the mining height is 3 m. The width of the entries and cross cut is 6.5 m. The chain pillars between the entries are 3 m high, 8 m wide and 26 m long.

The mining geometry is built in a 1000 m long, 240 m high, and 240 m wide block with graded mesh, as shown in Figure 2. The bottom layer in this figure represents half of the 3 m thick coal seam. The meshing at the central portion of the base of the block is made finer to in order to represent the entries and chain pillars in detail (Figure 3). Within the fine meshed region, MC interface separates the coal seam from the roof strata. The roof and floor strata are assumed to remain elastic throughout all stages of mining. The vertical planes bounding the block are free of shear stresses and horizontal

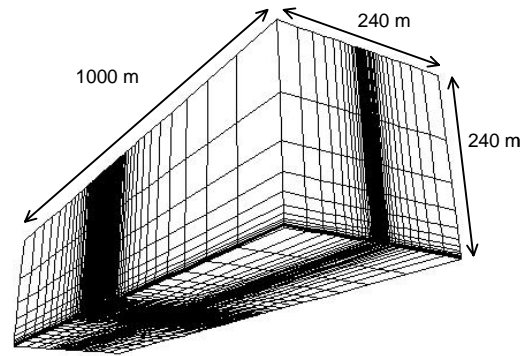


Figure 2. The FLAC^{3D} block model developed for longwall mining simulations.

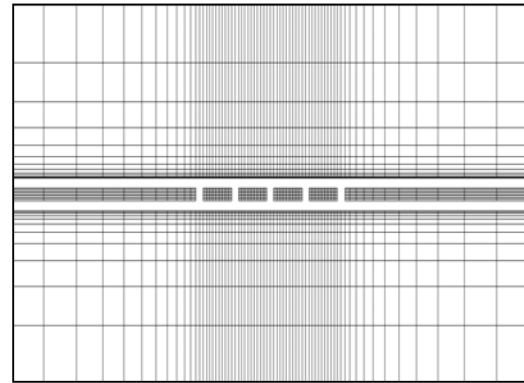


Figure 3. Bottom view of the FLAC^{3D} block model showing the fine mesh at the central area.

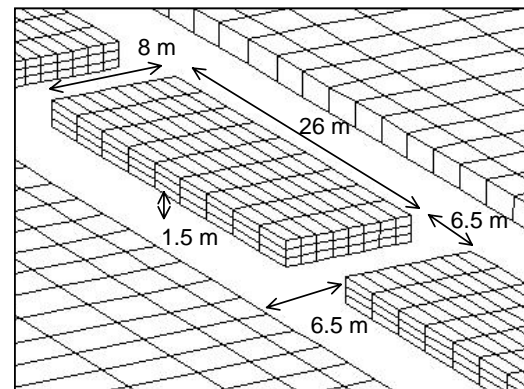


Figure 4. The entry system dimensions.

displacement. The horizontal plane at the base of the model, which is a plane of symmetry, is also free of shear stresses and subject to zero vertical displacement. The model is loaded at the top with a uniform vertical stress of 11 MPa to give a total overburden pressure of 17 MPa at the coal seam level. As seen in Figure 4, the element size in the chain pillars within the fine meshed central region is 1 m × 3 m × 0.5 m in the x, y and z-directions, respectively.

2.1 Determination of material properties

In addition to the peak cohesion, friction angle, and dilation angle in the MC model, the MCSS model also requires parameters describing the rate of cohesion and/or friction drop as a function of plastic strain in the post-peak region. The determination of the MC and MCSS parameters for a rock mass is a difficult task, but can be carried out empirically by performing back-analyses. In this study, the parameter determination is based on the two most commonly used empirical pillar strength formulas given by Salamon (1967) and Bieniawski (1984).

A FLAC^{3D} model of a single test pillar was developed to establish the most suitable combination of coal MCSS parameters for replicating pillar strength values based on empirical formulas. Figure 5 shows the FLAC^{3D} model of the test pillar in a room and pillar environment. By considering symmetry conditions, one quarter of the pillar is modeled. The vertical walls of the model are set as frictionless by fixing the normal displacements on them, except for pillar sides when they are formed. The model is loaded along the top boundary using a constant displacement of 2×10^{-7} m per FLAC step.

The floor material is modeled as an elastic layer having a 20 GPa elastic modulus. The MC interface between the pillar and floor has strength parameters of 0.5 MPa cohesion and friction angle of 23 degrees. For all pillar test simulations, the friction and dilation angles are held constant at 30 and 15 degrees, respectively.

Four pillar width-to-height (w/h) ratios (1, 2, 3, and 4) were modeled. For each w/h ratio, the numerical model was run with different combinations of a peak cohesion and cohesion drop rate.

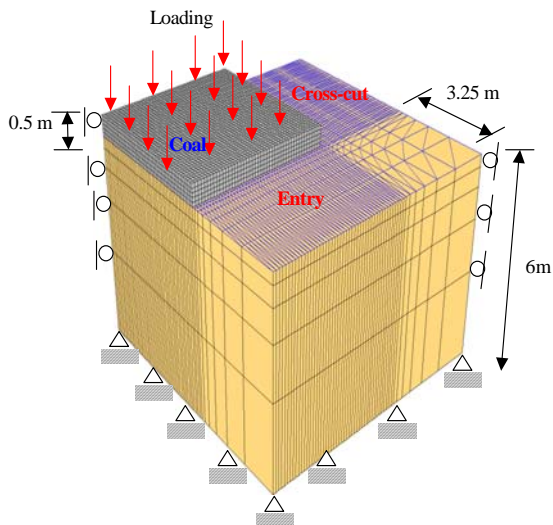


Figure 5. Test pillar model geometry.

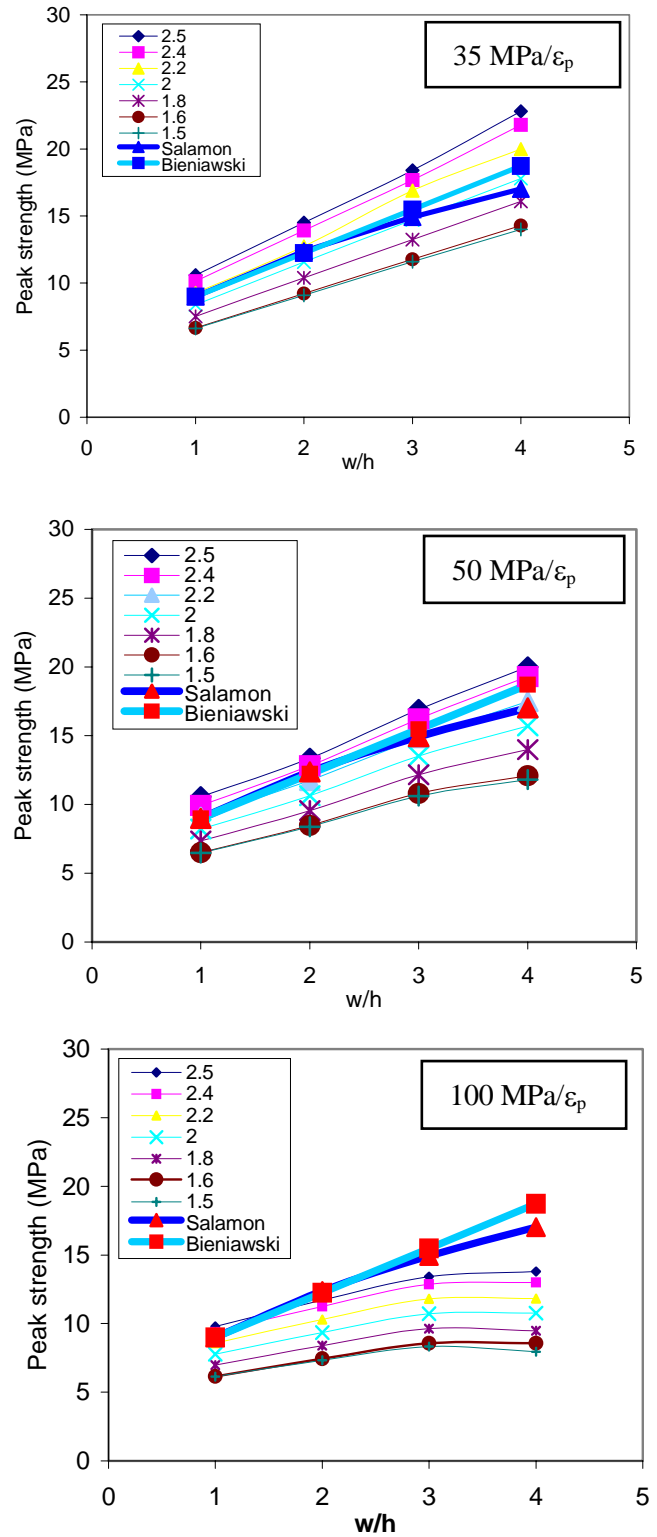


Figure 6. Model pillar strength versus empirical pillar strength at cohesion drop rates of 35, 50, 100 MPa/ε_p (Strength formulas: Salamon: $9(w^{0.46}/h^{0.66})$, Bieniawski: $9(0.64+0.36w/h)$ in MPa; assuming a coal cubic strength value of 9 MPa)

The strengths established from the test pillar models are plotted against the empirical pillar strength formulas in Figure 6 for the cohesion drop rates of 35, 50, and 100 MPa per plastic strain (ε_p) increment. Based on the trends of these plots, a

peak cohesion of 2.2 MPa and cohesion drop rate of 50 MPa/ ϵ_p is considered suitable for modeling yielding of the chain pillars.

The test pillar models were repeated using the MC failure criterion with the same peak cohesion, friction and dilation angle values as for the MCSS model. By averaging vertical stress and the vertical deformation histories across the top of the pillar, an overall stress-strain curve for an individual pillar could be obtained. Figure 7 shows such curves for pillar w/h ratios of 1, 2 and 3, using MC and MCSS criteria.

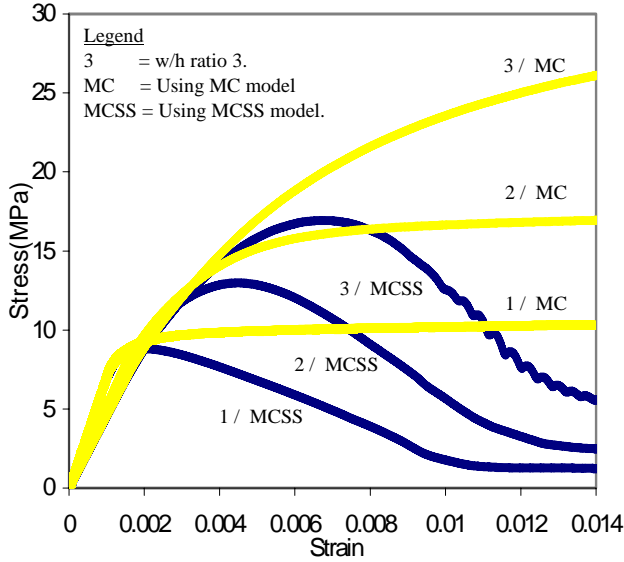


Figure 7. The vertical stress-strain curves of MC and MCSS pillars.

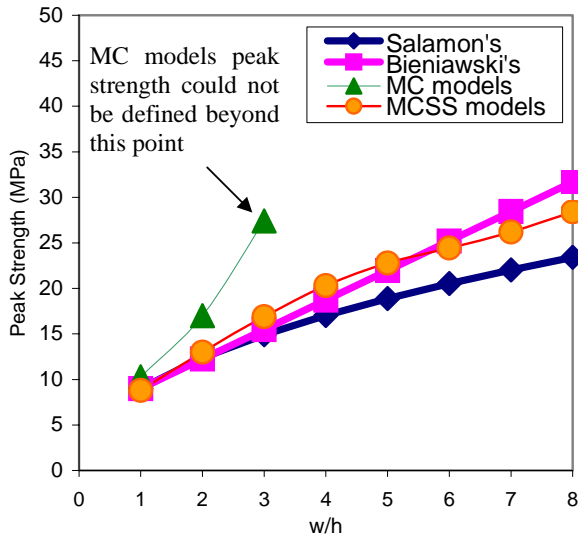


Figure 8. Pillar strength determination from numerical modeling and empirical formulas (refer to Figure 6 for empirical strength formulas)

The difference in pillar response is obvious; MC does not allow the true softening (no peak strength and no strength drop) and pillars maintain high residual strengths. On the other hand, MCSS models yield and reach much lower residual strengths. The pillar strength values, corresponding to both MC and MCSS materials, are plotted against the empirical pillar strength formulas of Salamon (1967) and Bieniawski (1984) in Figure 8. The MC model strengths tend to increase rapidly while MCSS model strengths follow the empirical strength trends, indicating that MCSS models give more realistic pillar stress-deformation curves than MC models

2.2 Gob compaction

The gob compaction process is an essential part of the longwalling process since it can alter the pillar and abutment loads by acting as an additional support for the system. The gob behavior is based on the following “compaction” model: vertical stress (σ_v) in the gob increases with increasing vertical strain (ϵ_v) according to the relationship given by Salamon (1990),

$$\sigma_v = \frac{a\epsilon_v}{b - \epsilon_v} \quad (1)$$

where “a” is gob initial deformation modulus; and “b” is the limiting vertical strain. Based on studies carried out at the USBM on gob behavior, the values for the constants were taken as $a=3.5$ MPa and $b=0.5$ (Deno and Mark 1993).

Two different algorithms are considered for implementation of the gob behavior of Eq.1 in the FLAC^{3D} model. In the first algorithm, referred to as the “nodal force”, the compaction load is modeled as the sum of vertical forces applied at the grid points of the roof elements in the back area after mining. After each mining step, the vertical strain in a particular zone within the gob area is used to calculate the vertical stress according to Eq. 1. Grid reaction forces are then calculated by multiplying vertical stress by the corresponding area of the roof element. In the second method, the gob is modeled as a non-linear elastic material. Its bulk modulus is continually increased as function of vertical strain within the gob area. The algorithm for this “modulus updating” method uses the bulk modulus K for each gob element:

$$K = \frac{1.75}{0.5 - \epsilon_z} \quad (2)$$

where ϵ_z is the vertical strain in the element (Badr et al. 2002).

Implementation of these two methods makes use of the “linked list” concept in FLAC^{3D}. The nodes (or zones) that will be replaced by gob material are defined by their addresses in a particular linked list. Then, using the FLAC^{3D} programming language ‘FISH’, a function updates the forces (or bulk modulus) of each node (or zone) using Eq. 1 or Eq. 2. After each mining step, the algorithm is executed in 50 step intervals until the model is brought to equilibrium (Badr 2003).

The gob compaction curves for the analytic solution (Salamon 1990) and the two FLAC^{3D} algorithms are compared in Figure 9. As shown, both nodal force and modulus updating algorithms compare well with the analytical model. Since the nodal force algorithm requires longer running time, the modulus updating method was embraced as the gob model for the FLAC^{3D} longwall simulations performed in this study.

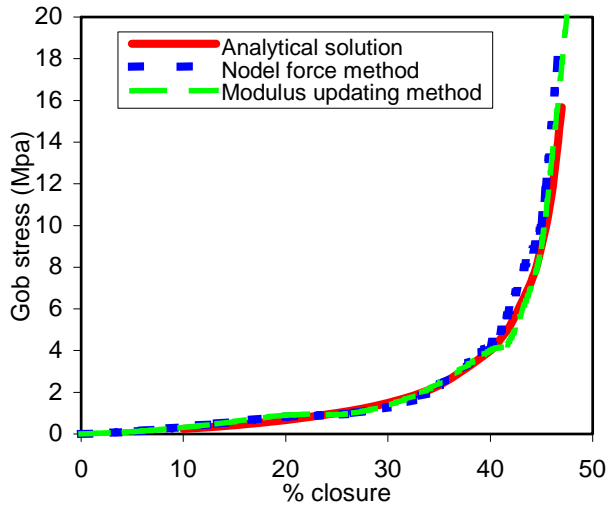


Figure 9. The gob stress-closure results from the analytical solution and two FLAC^{3D} algorithms.

3. RESULTS

Figure 10 defines the MCSS material parameters used in the model, which are also summarized in Table 1. For the coal seam, these parameters correspond to an MCSS material having a cubic strength of about 9 MPa, friction angle of 30 degrees, and cohesion drop rate of about 50 MPa/ ϵ_p .

The model of the longwall layout described in Section 2 is brought to equilibrium elastically to horizontal and vertical virgin stress conditions of 17 MPa at the coal seam level. The elastic coal seam is then replaced by a MCSS material prior to development. The entries are developed with the right entry leading the left entry by 9 m. The entries advance by 3 m in each mining step. A cross-cut is

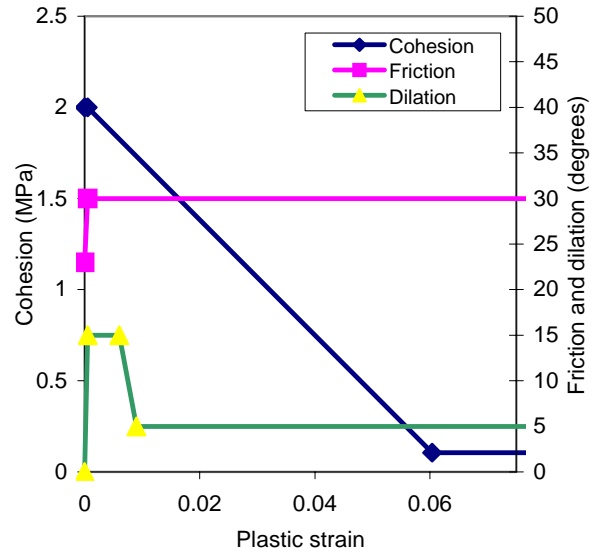


Figure 10. MCSS parameters used for modeling of the coal material.

Table 1. Material properties used in longwall simulations.

Property	Values
<u>Miscellaneous</u>	
Seam depth	680 m
Stress gradient	0.025 MPa/m
σ_x , σ_y and σ_z	17 MPa
<u>Coal properties</u>	
Coal elastic modulus	3 GPa
Coal Poisson's ratio	0.25
Coal strength	7.6 MPa
Coal Density	1313 Kg/m ³
<u>Roof properties</u>	
Elastic modulus	20 GPa
Poisson's ratio	0.25
Density	2500 Kg/m ³
<u>Interface properties</u>	
Type	Mohr-Coulomb
Cohesion	0.5 MPa
Friction angle	20°

then mined when the trailing entry is 9 m ahead. Mining of the longwalls is carried out starting at the right panel. The longwall advances initially in steps of 50 m and then the steps are reduced to 10 m in the fine-meshed central region of the model. After each longwall advance the area behind the longwall face is changed to “gob material” and the model is brought to equilibrium. The pillar response to mining is monitored using a FISH algorithm. The algorithm keeps a record of the vertical stress and vertical strain histories of all zones comprising the top of the pillar, and then averages these values to produce an average vertical pillar stress-strain curve. Figure 11 shows a typical pillar stress-strain curve

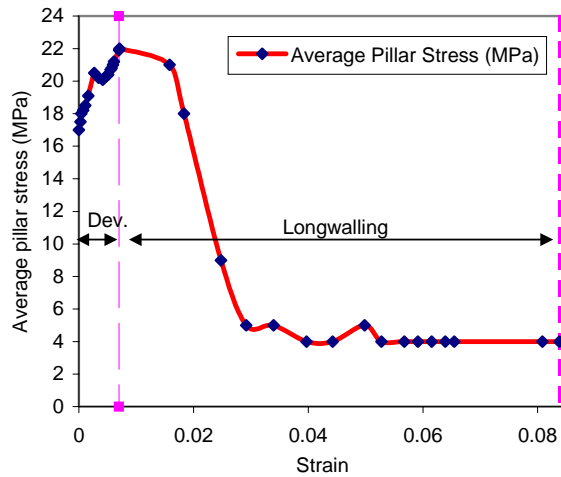


Figure 11. Complete average vertical stress-strain curve of the yielding chain pillar in modeled longwall layout.

obtained from the FLAC^{3D} simulation. The vertical dashed line shows the pillar loading at the end of entry development. At this stage, the pillar is at or close to its peak capacity. The pre-peak stress drops indicate sidewall failures experienced by the pillar during entry development. As the longwall approaches, the pillar initially sheds load slowly and subsequently rapidly, eventually reaching eight per cent compression. At its residual strength, the pillar carries a vertical stress of 4 MPa, which is considered sufficient for supporting the roof in two entry systems.

The pillar strength in the longwall model is more than that estimated by the test pillar model and empirical strength formulas. Further refinement of the strength parameters could be achieved by iterating on the contact and coal seam properties through parametric studies, which would involve six independent variables, not including parameters for the roof material. As was the case with the test pillar model, this iterative process would likely provide more than one set of parameters giving strength values similar to those predicted by the empirical strength formulas. Further studies in this area are needed to fine-tune the optimum parameter combination.

Figure 12 shows the gob compaction as mining progresses, referenced to a point at the center of the first panel. After mining of the first panel, the vertical stress in the gob is 1.8 MPa. The gob stress increases to the virgin stress level of 17 MPa after the second panel is mined.

The results from the longwall model are compared to in-situ measurements using borehole pressure cells (BPCs) from a mine with similar conditions (Schisler 2002). The FLAC^{3D} model shows that the

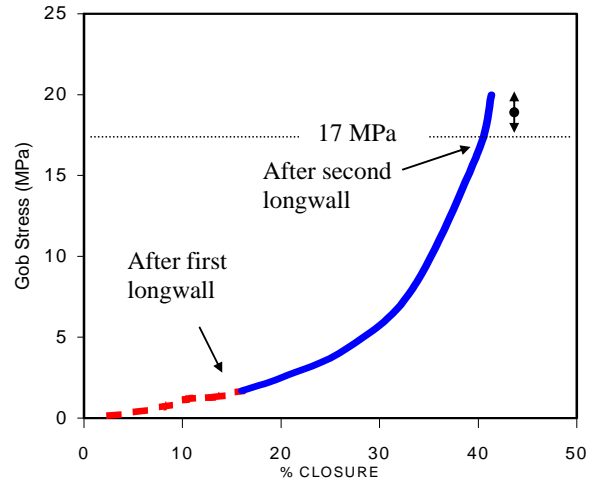


Figure 12. Vertical stress and closure induced at a point in the gob

pillar hardens to 22 MPa while the in-situ pillar monitoring showed 16 MPa during entry development. This difference is probably partly due to the selection of the model parameters as discussed above, and partly due to the installation sequence of the BPCs, which occurred after the pillar was developed, and thus did not completely capture the side wall loading by the approaching development faces. When the pillar yielded in the model, the longwall face was approximately 150 m from the pillar centerline. Although there is no in-situ load measurement available in pillars under similar situations, the authors' observations of intense pillar scaling in similar face positions in deep coal mines support the finding of the model.

3. CONCLUSIONS

A three dimensional model of a coal longwall mine is developed using FLAC^{3D}. The model incorporates mining stages, softening behavior of the coal seam, and gob compaction in the mined out area. The model results indicate that FLAC^{3D} is a suitable tool to aid in the design, evaluation, and performance assessments for complex longwall layouts.

The test pillar studies show that the Mohr-Coulomb Strain Softening model is more realistic than the traditional Mohr-Coulomb constitutive law for estimating the strength and post peak behavior of coal pillars.

The strain softening parameters developed in this study could be used as a starting point for modeling of coal seams. However, due to more than one combination of strength parameters giving the same rock mass strength value, and also mesh size

dependency of the program, it is advised that the strength parameters for a particular coal seam be developed on a case bases, using a back-analysis process similar to that described in the paper.

4. ACKNOWLEDGMENT

This publication was supported by Cooperative Agreement number U60/CCU816929-02 from the Department of Health and Human Services, the Center for Disease Control and Prevention (CDC). Its contents are solely the responsibility of the authors and do not necessarily represent the official views of the Department of Health and Human Services, CDC. Support provided by Department of Health and Human Services, CDC, is greatly acknowledged. The work presented is part of the Health and Safety research activities currently carried out at Western Mining Resource Center (WMRC) at the Colorado School of Mines.

5. REFERENCES

- Badr, S. A., Schissler, A., Salamon, M.D.G. Ozbay, U. 2002. Numerical Modeling of Yielding Chain Pillars in Longwall Mines. Proc. of the 5th North American Rock Mechanics Symposium, Toronto Canada. pp 99-107.
- Badr, S. A. (2003) Numerical Analysis of coal yield pillars at deep longwall mines. Ph .D. Thesis in preparation. Department of Mining Engineering, Colorado School of Mines, Golden, Colorado (To be submitted.).
- Bieniawski, Z.T., 1984. Rock Mechanics Design in Mining and Tunneling. A.A. Balkema, p. 1-272.
- Deno M. Pappas and Christopher Mark 1993. Behavior of Simulated Longwall Gob material. United States Department of the Interior, Bureau of mines, Report of investigation No. 9458.
- FLAC3D 2002. Itasca Inc. Minnesota.
- Deno M. Pappas and Christopher Mark 1993 (Behavior of Simulated Longwall Gob material) United States Department of the Interior- Bureau of mines- Report of investigation No. 9458.
- Salamon, M.D.G. (1990) Mechanism of caving in longwall coal mining. Paper in Rock Mechanics Contributions and Challenges Proceedings of the 31st US Symposium, Ed. W. Hustrulid and G. A. Johnson. Denver, Colorado, June 18-20, 1990. A.A. Balkema, 1990 page 161-168.
- Salamon, M.D.G.(1967). "A study of the strength of coal pillars." Journal of South Africa Institute of Mining and Metallurgy, v. 68, p. 55-67.
- Schissler, A. 2002. Yield pillar design in non-homogenous and isotropic stress fields for soft minerals. Ph .D. Thesis. Department of Mining Engineering, Colorado School of Mines, Golden, Colorado.